HHS Public Access

Author manuscript

Cell. Author manuscript; available in PMC 2016 May 04.

Published in final edited form as:

Cell. 2012 May 11; 149(4): 886–898. doi:10.1016/j.cell.2012.02.062.

Inverse synaptic tagging of inactive synapses via dynamic interaction of Arc/Arg3.1 with CaMKIIβ

Hiroyuki Okuno[1,6,*], **Kaori Akashi**[3], **Yuichiro Ishii**[1,2], **Nan Yagishita-Kyo**[1,2], **Kanzo Suzuki**[1,2], **Mio Nonaka**[1,2,6], **Takashi Kawashima**[1,2], **Hajime Fujii**[1,6], **Sayaka Takemoto-Kimura**[1,5], **Manabu Abe**[3], **Rie Natsume**[3], **Shoaib Chowdhury**[4], **Kenji Sakimura**[3,6], **Paul F. Worley**[4], and **Haruhiko Bito**[1,2,6,*]

[1]Department of Neurochemistry, Graduate School of Medicine, The University of Tokyo, Bunkyo-ku, Tokyo 113-0033, Japan

[2]the Global Center of Education and Research for Chemical Biology of the Diseases, Graduate School of Medicine, The University of Tokyo, Bunkyo-ku, Tokyo 113-0033, Japan

[3]Department of Cellular Neurobiology, Brain Research Institute, Niigata University, Niigata 951-8585, Japan

[4]Department of Neuroscience, Johns Hopkins University School of Medicine, Baltimore, Maryland 21205, USA

[5]PRESTO-JST, Kawaguchi, Saitama 332-0012, Japan

[6]CREST-JST, Chiyoda-ku, Tokyo 102-0076, Japan

Summary

Arc/Arg3.1 gene product is rapidly upregulated by strong synaptic activity and critically contributes to weakening synapses by promoting AMPA-R endocytosis. However, how activity-induced Arc is redistributed and determines the synapses to be weakened remains unclear. Here, we show targeting of Arc to inactive synapses, via a high affinity interaction with CaMKIIβ that is unbound to calmodulin. Synaptic Arc accumulated during inactivity that followed strong activation, and correlated with removal of surface GluA1 from individual synapses. A lack of CaMKIIβ either *in vitro* or *in vivo* resulted in loss of Arc up-regulation in the silenced synapses. The discovery of Arc's role in “inverse synaptic tagging” that is specific for weaker synapses and prevents undesired enhancement of weak synapses in potentiated neurons, provides a new framework that reconciles essential roles of Arc both for the late phase of long-term plasticity and for reduction of surface AMPA-Rs in stimulated neurons.

[*]Corresponding authors: hbito@m.u-tokyo.ac.jp or okuno@m.u-tokyo.ac.jp.

Introduction

An outstanding challenge in neuroscience is the identification and characterization of neuronal activity-regulated genes that critically govern the molecular and cellular events underlying memory formation and processing (Bito et al., 1996; Flavell et al., 2006; Nedivi et al., 1993; Qian et al., 1993; Worley et al., 1993). The neuronal immediate early gene *Arc* (also called *Arg*3.1) is among the most promising candidates for such memory regulatory genes, as it is dynamically regulated, and its induction highly correlates with augmented neuronal activity that is required for cognitive processes such as spatial learning and memory consolidation (Guzowski et al., 1999; Link et al., 1995; Lyford et al., 1995; Ramirez-Amaya et al., 2005). Consistent with such an activity-dependent Arc up-regulation, the knockdown or knockout (KO) of *Arc* in rodents causes impairments in the persistence of long-term memory (Guzowski et al., 2000; Plath et al., 2006; Ploski et al., 2008) and in stimulus selectivity or experience-dependent cortical plasticity in the visual cortex (McCurry et al., 2010; Wang et al., 2006).

A large part of *Arc* function occurs postsynaptically. Biochemical and electron microscopy (EM) studies showed presence of Arc protein in the postsynaptic density (PSD) of activated neurons (Chowdhury et al., 2006; Moga et al., 2004). In the PSD, Arc interacts with the endocytic proteins endophilin and dynamin, and enhances the removal of AMPA-type glutamate receptors (AMPA-Rs) from the postsynaptic membrane (Chowdhury et al., 2006). This function, together with the activity-dependent expression of *Arc*, is implicated in several forms of protein translation-dependent synaptic long-term depression (LTD) (Park et al., 2008; Plath et al., 2006; Smith-Hicks et al., 2010; Waung et al., 2008) and homeostatic plasticity/synaptic scaling (Béïque et al., 2011; Chowdhury et al., 2006; Peebles et al., 2010; Rial Verde et al., 2006; Shepherd et al., 2006). This role of *Arc* in the cell-wide weakening of glutamatergic synaptic strength, however, is difficult to reconcile with a large amount of evidence that *Arc* is most strongly induced by stimuli that evoke long-term potentiation (LTP) (Link et al., 1995; Messaoudi et al., 2007; Moga et al., 2004; Ying et al., 2002), and that both *Arc* mRNA and protein accumulate in the dendritic areas that receive high-frequency synaptic inputs (Moga et al., 2004; Steward et al., 1998). Such incongruity still remains because we critically lack knowledge about the molecular mechanisms of Arc association to PSD regions.

In this study, we have investigated the potential role of CaMKIIβ in determining the targeting of synaptic activity-induced Arc protein from the soma to individual synapses, and demonstrate a novel “inverse synaptic tagging” mechanism whereby an interaction between Arc and CaMKIIβ operates as a specific sensor for the inactive synapse-specific control of AMPA-R clearance at weaker synapses in potentiated neurons, based on a local history of both activity and inactivity.

Results

Arc directly interacts with CaMKIIβ in dendritic spines

A yeast two-hybrid screen was carried out to isolate putative postsynaptic Arc-binding proteins (Chowdhury et al., 2006). The screening yielded the β-isoform of CaMKII

(CaMKIIβ) as a binding partner candidate, and this binding was confirmed by an *in vitro* co-immunoprecipitation assay (Figure S1A). In hippocampal CA1/CA3 cell cultures, Arc immunoreactivity (IR) co-localized with CaMKIIβ IR in the dendritic spines of Arc-expressing neurons (Figure 1A). Furthermore, Arc IR was immunoprecipitated with an anti-CaMKIIβ antibody in brain lysates from wild type, but not from CaMKIIβ-knockout, mice (Figure 1B and S1B), indicating that Arc and CaMKIIβ are complexed in the brain. Arc-CaMKIIβ association was further tested *in situ*, using fluorescence resonance energy transfer (FRET) between CFP-tagged Arc (Arc-CFP) and YFP-tagged CaMKIIβ (CaMKIIβ-YFP). Arc-CFP showed a significant FRET with CaMKIIβ-YFP in spines of living hippocampal neurons treated with TTX ($p < 0.0001$, Figure S1C), but not with other tagged PSD proteins, such as CaMKIIα-YFP and Homer1c-YFP, suggesting a high specificity for Arc-CaMKIIβ interaction.

High affinity Arc-CaMKIIβ binding in the absence of Ca^{2+} and its suppression by Ca^{2+}/CaM

We next investigated the biochemical properties of Arc-CaMKIIβ interaction. A GST pull-down experiment confirmed direct binding between recombinant Arc and CaMKIIβ. This interaction was strong in the absence of Ca^{2+} and calmodulin (CaM) but was attenuated when Ca^{2+}/CaM was present (Figure 1C and S1D). In contrast, an Arc-CaMKIIα interaction was observed only in the presence of Ca^{2+}/CaM (Figure S1E). The CaM-binding inhibitor W-7 reversed the effects of Ca^{2+}/CaM (Figure S1F). Based on Scatchard analyses, the measured affinity between Arc and CaMKIIβ was indeed high (∼0.9 μM) in the absence of Ca^{2+}/CaM; it decreased by 7-fold in the presence of Ca^{2+}/CaM (Kd, ∼6 μM) (Figure 1D). In contrast, Arc-CaMKIIα interactions showed a much lower affinity (Kd, ∼10 μM with Ca^{2+}/CaM; ∼60 μM without Ca^{2+}/CaM) (data not shown). These results, together, suggested that Arc preferentially binds to CaMKIIβ in a Ca^{2+}/CaM-unbound, inactive, state.

Arc is more enriched in the PSD during synaptic inactivity following de novo transcription-inducing stimuli in cultured neurons

This raised the possibility that Arc synaptic localization could be regulated by synaptic activity *and* inactivity through modulation of Ca^{2+}/CaM binding to CaMKIIβ. We directly tested this, by application of *de novo* transcription-inducing stimuli, and then monitoring newly synthesized Arc protein at the PSD, after maintaining or shutting down synaptic activity. Cultured hippocampal CA1/CA3 neurons were pretreated with tetrodotoxin (TTX) until pre-existing Arc protein was cleared (Figure S2A), and then stimulated by BDNF application for 2 h, similar to a protocol that has been shown to induce strong CA1-LTP accompanied by new Arc induction (Ying et al., 2002). Immediately after BDNF activation, new synthesis of Arc protein was strongly induced (Figures S2A, S2B, and S2C). Arc IR was mainly associated with the dendritic shaft, although a minority was present in the PSD (Figure 2A, BDNF). Additional incubation with a basal medium caused little change in Arc localization (Figure 2A, BDNF->no drug). However, when spontaneous synaptic activity was blocked with TTX after the BDNF treatment, Arc IR intensity in the PSD became much more pronounced (Figure 2A, BDNF->TTX). Though surprising and counterintuitive, this finding was in accordance with the biochemical binding data which favored Arc association to inactive CaMKIIβ. To compare data across different conditions, we calculated an Arc accumulation index by normalizing spine Arc expression levels to the adjacent dendritic

shafts (see Experimental procedures). Based on this index, we found little change between "no drug after BDNF" and "BDNF after BDNF" conditions (Figure 2B, BDNF->no drug and BDNF->BDNF). In contrast, either "BDNF->TTX" or "BDNF->CNQX/AP5" treatment, which inhibits glutamatergic transmission pre- or post-synaptically, caused a significant rightward shift in the synaptic Arc distribution (Figure 2B, $p < 0.0001$, Kolmogorov-Smirnov (K-S) test). Enhancing glutamatergic synaptic activity using a cocktail of the $GABA_A$ receptor antagonist bicuculline and a presynaptic potassium-channel blocker, 4-aminopyridine, (BIC/4AP) had little effect (Figure 2B, BDNF->BIC/4AP). Consistent with these results, after activity blockade, the absolute Arc IR was enriched in the PSD, whereas the shaft IR decreased, thus creating an Arc gradient that favored synaptic Arc (Figure S2D). Consistent with this sensitivity to inactivity, Arc IR intensity exhibited a significantly higher coefficient of variation in individual PSDs of neurons expressing Arc under a basal medium condition, compared to that of another PSD protein, Homer (Figure S2E).

Taken together, these results pointed to the surprising possibility that perhaps individual history of synaptic inactivity, but not enhanced activity, contributed to the synaptic pool of newly-induced Arc protein.

Essentially similar results were obtained using neuronal cultures of hippocampal dentate gyrus (DG), which are known to express the highest amounts of activity-induced *Arc* mRNA and proteins (Link et al., 1995; Lyford et al., 1995; Steward et al., 1998). BIC/4AP treatment for 2 h induced strong expression of newly translated Arc in our DG neuron culture (Figure S3A), and a subsequent follow-up treatment with TTX for an additional 2 h (BIC/4AP->TTX 2 h, $p < 0.0001$, K-S test), but not with BIC/4AP (BIC/4AP 4 h), caused an increase in synaptic Arc (Figures S3B and S3C). This inactivity-induced enrichment was further promoted when TTX duration was extended to 4 h ($p < 0.001$, K-S test for BIC/4AP 2 h->TTX 2 h vs BIC/4AP 2 h->TTX 4 h), whereas BIC/4AP follow-up for 4 h (BIC/4AP 6 h) had little effect (Figure S3B). In contrast, no such enrichment was observed for PSD-95 (data not shown).

Increased synaptic Arc maintenance is induced by single-synapse inactivation

To discriminate whether Arc protein dynamics reflected the degree of local synaptic inactivity of individual synapses rather than the degree of general, cell-wide activity or inactivity, we suppressed synaptic activity on a single-synapse basis by expressing doxycycline-inducible GFP-tagged tetanus-toxin (GFP-TeNT) presynaptically, resulting in cleavage of VAMP2 and blocking neurotransmitter release in the GFP-labeled axon (Figure 2C) (Yamamoto et al., 2003). To ensure scoring of the effect of TeNT on excitatory, but not inhibitory, synapses, BDNF-induced Arc IR was measured only in PSD-95 containing dendritic spines in hippocampal CA1/CA3 neurons. The Arc IR at spines contacting GFP-TeNT-positive axons was significantly higher than those at adjacent spines that were juxtaposed to GFP-TeNT-negative boutons (Figures 2C and 2D). Such an inactive synapse-restricted regulation was not observed for PSD-95 IR (Figure 2E). Similar results were obtained using DG granule cells activated with BIC/4AP (Figure S3D). Local synaptic inactivity thus directly controls spine Arc dynamics in a synapse-autonomous manner.

Time-lapse imaging of synaptic accumulation of Arc during inactivity

To examine the single spine kinetics of Arc dynamics exposed to synaptic inactivity after Arc induction, we developed a live Arc protein-reporter imaging system in which activity-dependent expression and synaptic targeting of Arc protein were monitored over time in the same dendritic spines. A monomeric EGFP-tagged Arc (mEGFP-Arc) was driven under the control of the 7-kb Arc promoter (Kawashima et al., 2009) in hippocampal neurons along with a volume-filling RFP that was constitutively expressed. The initial mEGFP-Arc distribution after a 2-h BDNF treatment recapitulated the distribution of endogenous Arc IR; the mEGFP-Arc signals were mainly observed in the dendritic shafts, and minor pools of the signal were detected in some spines (Figure 3A, left panels; also see Figure 2A). We found that mEGFP-Arc signals accumulated more in dendritic spines than in shafts after cessation of activity in TTX (Figure 3A, upper panels), but not when spontaneous activity remained (Figure 3A, lower panels). Volume-normalized mEGFP-Arc intensity in individual spines also revealed significant increases over time during synaptic inactivity (Figure 3B) ($p < 0.003$, K-S test).

We further carried out dual-color live imaging of constitutively expressed mEGFP-tagged CaMKIIβ (mEGFP-CaMKIIβ) and activity-driven mCherry-tagged Arc (mCherry-Arc) (Figure 3C). We choose an experimental condition under which BDNF 2-h treatment strongly induced new expression of mCherry-Arc from the Arc 7-kb promoter while it evoked little dynamic translocation of mEGFP-CaMKIIβ (Figures 3C and 3D). Interestingly, ensemble data revealed that at 2 h after TTX treatment, the quantity of spine mCherry-Arc during TTX treatment positively correlated with that of spine mEGFP-CaMKIIβ, but not at 30 min after BDNF treatment (Figure 3E). This suggested that Arc accumulation in a spine during a period of inactivity might be determined by the CaMKIIβ level in the spine at the start of the inactivity period.

Effects of inactivity-enhanced Arc synaptic localization on GluA1 surface expression

Previous studies showed that Arc interacted with the endocytic machinery and regulated the trafficking of the GluA1 subunit of AMPA-R (Béïque et al., 2011; Chowdhury et al., 2006; Rial Verde et al., 2006; Shepherd et al., 2006). Consequently, we examined whether preferential Arc maintenance at individual inactive postsynapses may help control GluA1 surface expression levels (Figure 4).

When hippocampal CA1/CA3 neurons were treated with BDNF for 2 h, surface expression levels of synaptic GluA1 significantly increased ($p < 0.001$, Figure 4A), consistent with generalized BDNF-LTP in previous reports (Caldeira et al., 2007; Ying et al., 2002). Surface GluA1 levels slightly decreased, but remained significantly high, during a follow-up incubation period in the presence of BDNF or without any drugs ($p < 0.05$, Figure 4A, right panel): a decaying component of surface GluA1 levels may be accounted for by an activity-dependent regulation of surface receptor degradation at active synapses. When BDNF-treated neurons were subsequently treated with TTX for 2 h, surface GluA1 expression levels were markedly reduced to the levels observed prior to BDNF activation (Figure 4A, $p < 0.05$, BDNF->TTX vs 'BDNF->BDNF' or 'BDNF->no drug'; not significant, BDNF->TTX vs 'no activation'). Because cell-wide Arc expression levels determined by Western

blot did not differ among these follow-up treatment groups (Figure S4A), the reduction in surface GluA1 levels at synapses may not directly correlate with global Arc expression *per se*, but may reflect local synaptic Arc dynamics directly associated with local synaptic activity/inactivity. Strikingly a clear negative correlation was invariably detected at single synapses between the amounts of surface GluA1 and Arc IR that were co-adjacent to the presynaptic marker vGlut1 (Figures 4B-D). As a follow-up experiment of Figure 2C, we also measured surface GluA1 levels in spines that faced TeNT-expressing axons and compared them to those in adjacent non-silenced spines (Figure S4B). The GluA1 levels were significantly lower in spines close to the TeNT axons than in neighboring control spines ($p < 0.05$) while control GFP expression had no effect (Figure S4C).

These results provide compelling evidence that the degree of maintenance of newly induced Arc protein in the synaptic pool quantitatively determines the turnover of GluA1 in an input-specific manner. Furthermore, the down-regulation of GluA1 in Arc-containing synapses, but not in Arc-deficient synapses, is consistent with the idea that an inactivity-modulated concentration gradient of Arc plays a role in facilitating the clearance of initially up-regulated GluA1 from weak synapses during the late phase of various forms of synaptic potentiation.

CaMKIIβ acts as a scaffold for Arc in dendritic spines

Because CaMKIIβ was enriched at dendritic spines (Figures 1A and 3C) and because we found evidence for the physical proximity and association between CaMKIIβ and Arc (Figures 1B, 1D, S1A and S1C), we determined the effects of CaMKIIβ knockdown (using a short hairpin (sh) RNA vector) on Arc accumulation in the dendritic spines of neurons treated with BDNF followed by TTX (Figures 5A-C). A line-profile of fluorescence intensity from the tip of spine to the adjacent dendritic shaft revealed that Arc IR preferentially accumulated at the spines in mock-control cells (sh nega). In contrast, CaMKIIβ knockdown (sh beta) effectively suppressed Arc accumulation in the spines (Figures 5A and 5C). This CaMKIIβ knockdown effect was not replicated by CaMKIIα knockdown (sh alpha), but could be rescued by co-expressing an RNAi-resistant wild-type CaMKIIβ (sh beta + CaMKIIβ-WTres) (Figures 5B and 5C). Thus, the shRNA effect on Arc localization is genuinely mediated by a loss of CaMKIIβ (Figure 5C and Figure S5A). The specificity and efficacy of the CaMKII knockdown using our shRNA vectors were confirmed by immunostaining (Figure S5B). Similar analyses on another PSD protein, Homer, showed that Homer accumulation in the spines was unaltered with either CaMKIIβ or CaMKIIα knockdown (Figures S5C and S5D), ruling out a general disruption of PSD organization by CaMKIIβ knockdown.

We next performed a series of rescue experiments using several RNAi-resistant CaMKIIβ mutants (Figures 5D and S6A). Expression of a kinase-dead and autophosphorylation-deficient mutant K43M/T287Ares was as effective as WTres CaMKIIβ in rescuing the deficit in synaptic Arc accumulation caused by CaMKIIβ knockdown ($p < 0.01$). In contrast, a phospho-mimic, constitutively active mutant T287Dres was capable of rescuing to the some extent, but not fully, the deficit in the synaptic Arc localization ($p < 0.05$ versus WT by K-S test, but also $p < 0.05$ versus the empty control by ANOVA with Tukey's test). In

keeping with these neuronal *in situ* results, *in vitro* GST binding assays showed that a recombinant K43M/T287A (as well as a T287A) mutant protein showed strong Arc-binding in the absence of Ca^{2+}/CaM to the same extent as a WT CaMKIIβ protein (Figures S6B and S6C), suggesting that the kinase activity *per se* does not contribute to Arc binding to CaMKIIβ. In contrast, a T287D mutant protein showed a much weakened, but residual, binding activity (Figure S6B). Since these results suggested the critical importance of the CaM-unbound closed conformation (Hudmon and Schulman, 2002) for Arc-binding, we specifically tested this idea and found that expression of a constitutive CaM-binding-deficient mutant A303Rres was sufficient to restore synaptic Arc accumulation (Figure 5D). Interestingly a recombinant protein of a non-F-actin binding CaMKIIβ isoform βe exhibited an *in vitro* Arc binding activity similar to that of WT CaMKIIβ protein (Figure S6D), yet its expression only partially rescued the CaMKIIβ knockdown phenotype (Figure 6D). Overall, this is consistent with the idea that F-actin-binding may be necessary for synaptic targeting of WT CaMKIIβ, but perhaps not directly for Arc accumulation *per se*. Taken together, these results strongly support the notion that activity-induced Arc is anchored at synapses through its interaction with a CaM-unbound CaMKIIβ during inactivity.

Increased Arc maintenance in the postsynapses after cortical activity blockade in vivo

We then asked whether the *in vitro* observations described above were relevant *in vivo*. To test this, we generated transgenic (Tg) mice in which mEGFP-Arc was driven by the Arc promoter (Figures S7A and S7B). We took advantage of the contralaterality of the mouse visual system to physiologically manipulate cortical activity/inactivity in a manner analogous to the above *in vitro* experiments, while keeping rigorous within-individual controls (Figures 6A and 6B). Following dark-rearing, mice were exposed to light on both eyes for 4 h to trigger strong bilateral activation of the primary visual cortex (V1); the neuronal activity of one V1 hemisphere was then shut off by injecting TTX into one eye, whereas the other eye was injected with PBS as a control (Figures 6A and 6B). Two control experiments were carried out. In the first control experiment, we confirmed that a similar intraocular TTX injection before light exposure effectively prevented V1 activation as shown by the lack of mEGFP-Arc induction after this procedure (Figure S7C). In the second control experiment, we tested whether the overall expression levels of the Arc protein reporter that was induced during the 4-h light exposure was altered by an unilateral silencing due to monocular TTX injection, and we found that, similar to our *in vitro* observations, the *overall* degree of mEGFP-Arc induction did not differ between the two hemispheres (Figure 6B). Having ascertained these controls, we then blindly quantified the expression levels of *synaptic* mEGFP-Arc in both hemispheres by measuring GFP IR in PSD-95-positive PSDs with high power microscopy (Figure S7D), and compared the intensity distributions between the experimental and control hemispheres (Figures 6C and 6D). The synaptic mEGFP-Arc signals were found to be significantly higher in the hemisphere that was contralateral to the TTX-treated eye as opposed to the control ipsilateral one ($p < 0.001$, paired t-test) (Figure 6D). No such difference was detected for the levels of PSD-95 IR (Figure S7E).

We further assessed the inactivity-dependent regulation of synaptic Arc levels in a CaMKIIβ-null genotype *in vivo*, with the same experimental paradigm, using a cross of the CaMKIIβ-KO and the mEGFP-Arc reporter Tg mouse line. Blind analysis showed no

difference in mEGFP-Arc levels in the PSD in the V1 between the silenced and control hemispheres, in the mEGFP-Arc Tg/CaMKIIβ-null combined genotype (Figure 6E). The distribution of PSD-95 IR was not significantly altered between hemispheres, either in the wild-type or in the CaMKIIβ-KO (Figures S7E and S7F), in keeping with a prior anatomical observation in CaMKIIβ-null mice that reported little change in synaptic morphology (Borgesius et al., 2011).

Taken together, these *in vivo* results provide strong evidence that activity-induced Arc protein is preferentially targeted to inactive CaMKIIβ at weak synapses as a consequence of the sequential history of synaptic activity and inactivity in the brain.

Preferential Arc targeting into weak synapses following plasticity-inducing stimulation

Our data suggested that Arc protein is anchored in less active synapses through its interaction with an inactive form of CaMKIIβ. Is activity-induced Arc then directed less to potentiated synapses and more to non-potentiated synapses following plasticity-inducing stimulation? We tested this notion, in cultured neurons expressing a volume marker RFP and activity-regulated mEGFP-Arc. We applied high-frequency electrical field stimulation that evoked stimulus-induced volume expansion in a large population of spines (Figures 7A). Following stimulation, the emerging fluorescence from newly synthesized mEGFP-Arc could be co-imaged in a sizable proportion of synapses along with volume expansion, a reliable index of synaptic potentiation (Matsuzaki et al., 2004) (Figure 7C, see also Supplemental Movie). When spines were classified into “expanded” and “non-expanded” groups (see Experimental procedures), the expanded group showed robust and long-lasting increases (> 3 h), while the volume of the non-expanded group remained stable (Figure 7C). Analysis of the volume-corrected mEGFP-Arc level in single spines raised the possibility that high levels of mEGFP-Arc were found in non-expanded, rather than expanded spines at 3 h after the stimulation (Figure 7B). Indeed, the mEGFP-Arc levels significantly increased between 2 h and 3 h after the onset of the stimulation in the non-expanded group ($p = 0.016$), but not in the expanded group (Figure 7D).

Taken together, our data are consistent with an inverse synaptic tagging role of activity-induced Arc, in which Arc is much more targeted to less active synapses than to expanded, potentiated synapses, during the late phase of synaptic potentiation (Figure 7E).

Discussion

Clearance of up-regulated GluA1 in inactive synapses, via a local inactivity-controlled recruitment of Arc that relies upon a prominent structural role of inactive CaMKIIβ as a PSD scaffold

We here demonstrated that the level of local synaptic *in*activity critically determines the kinetics of activity-induced Arc turnover at the synapse. We further discovered that this mechanism is made possible by a heightened affinity between an inactive form of CaMKIIβ and Arc at synapses, which allows Arc to be preferentially maintained at inactive synapses rather than active synapses. Arc targeting to less active synapses via CaMKIIβ thus provides

a tunable mechanism for synapse-specific control of AMPA-R trafficking according to the history of local synaptic activity and inactivity.

Our results demonstrate that an inactive form of CaMKIIβ, rather than CaMKIIα, has a more dominant role in Arc regulation at synapses in neurons, both *in vitro* and *in vivo*, especially under synaptically silenced conditions following Arc induction. We cannot, however, rule out a possible role for CaMKIIα in Arc regulation under other conditions (Donai et al., 2003).

Previously, CaMKIIβ, together with CaMKIIα, was shown to translocate into the spines from the dendritic shaft upon strong synaptic inputs (Shen and Meyer, 1998). Our finding that Arc preferentially binds to inactive CaMKIIβ suggests that the α/β ratio in a heteromeric CaMKII complex may play a determinant role in enabling the CaMKII complex to retain Arc in the spines. While it remains to be shown how the history of the spine's activity exactly specifies the composition of the CaMKII complex, a role for local translation of CaMKIIα has previously been proposed (Miller et al., 2002). Overall, at the single spine level, the dynamics of the synaptic CaMKII complex might provide the basis for assigning the late outcome of plasticity, perhaps as a function of an enhanced CaMKIIα protein synthesis (in strongly stimulated (late LTP-like) spines), or via a privileged CaMKIIβ-Arc interaction (in weakly stimulated (early LTP-like) spines). As the majority of inactive CaMKIIβ reside in the dendritic shaft, further studies are needed to elucidate key mechanisms that allow Arc to preferentially interact with a specific pool of inactive CaMKIIβ that resides within the spines.

Structurally, CaMKIIβ has a unique F-actin-binding insertion between the regulatory and association domains (O'Leary et al., 2006; Okamoto et al., 2007; Shen and Meyer, 1998). We found that the same condition that favors an F-actin-CaMKIIβ complex formation, namely the absence of Ca^{2+}/CaM (O'Leary et al., 2006; Okamoto et al., 2007), also promotes Arc interaction with an inactive CaMKIIβ (Figure 1). However, an F-actin binding insertion in CaMKIIβ was dispensable for Arc binding (Figure S6). These observations imply that, while a sustained level of low Ca^{2+} concentration during synaptic inactivity would be consistent with the co-stabilization of both F-actin-CaMKIIβ and Arc-CaMKIIβ complexes within the synapses, the two complexes may be separable.

Capturing of Arc by CaMKIIβ: a novel mechanism for an inverse synaptic tagging process that operates at inactive synapses during late phase plasticity

The synaptic tagging and capture theory has recently provided an attractive framework that accounts for the persistence in the late phase of long-term, synapse-specific, macromolecule-synthesis-dependent forms of neuronal plasticity (Frey and Morris, 1997; Redondo et al., 2010). Although several candidate molecules and signaling pathways have been proposed as synaptic tags or active-synapse-targeted plasticity related proteins (PRPs), the relevant combination of synaptic tags in the potentiated spines and of the captured PRPs, to date, remains largely unknown (Navakkode et al., 2004; Okada et al., 2009; Redondo et al., 2010). Our results indicate an alternative, non-mutually exclusive, possibility. In this scenario, “inverse tags” may be specifically generated to sort newly synthesized PRPs to inactive synapses through an *in*activity-sensing mechanism. The selective avoidance of actively

tagged synapses by a negative plasticity factor, such as Arc, via a preferential interaction with an “inverse tag”, such as an inactive CaMKIIβ, may thus be considered the conceptual opposite of the classical notion of synaptic tagging, or an “*inverse synaptic tagging*” process. Preventing undesired synaptic enhancement at weak synapses, while sparing potentiated synapses, will ensure that the contrast between strong and weak inputs remains stable over time (Figure 7E).

Previous studies have established that activity-induced *Arc* mRNA and protein are enriched in dendritic regions in the DG that receive layer-specific, high-frequency stimulation (Steward et al., 1998; Moga et al., 2004). It has thus been widely assumed, though not directly tested, that Arc may be targeted to potentiated/stimulated synapses. Our results suggest that the actual sites of the Arc accumulation in previous studies might have been inactive synapses and/or in dendritic shafts within the activated areas. The role of Arc at less active synapses may readily reconcile apparently contradictory roles of Arc during the late-phase of various forms of long-term synaptic plasticity and during homeostatic plasticity and synaptic scaling (Chowdhury et al., 2006; Rial Verde et al., 2006; Shepherd et al., 2006). Our findings are also in keeping with an activity-dependent degradation of Arc through Ube3a, which may also contribute to the exclusion of Arc in active synapses (Greer et al., 2010).

The presence of such dual mechanisms for Arc regulation would be an effective way to achieve late-phase consolidation of the synaptic weight differences between active and inactive synapses following a strong synaptic potentiation (Figure 7E), such as during late-phase LTP or sharpening of sensory-evoked response tuning in the neocortex (McCurry et al., 2010; Wang et al., 2006). Our findings pave the way for elucidating the role of the signaling from the nucleus to synapses at unprecedented resolution and help advance our understanding of the information processing role of activity-dependent genes at single synapses.

Experimental Procedures

Plasmids and antibodies

Detailed information regarding plasmids and antibodies used in this work is described in the Extended Experimental Procedures.

Animals

Sprague-Dawley (SD) rats were used for neuronal culture preparation. A line of transgenic (Tg) mice harboring the Arc-promoter mEGFP-Arc was generated by microinjection of a mEGFP-Arc cDNA construct into fertilized C57BL/6 mouse eggs. Gene targeting of CaMKIIβ was carried in the C57BL/6-derived ES cell line RENKA (Mishina and Sakimura, 2007) by homologous recombination. Detailed characterization of CaMKIIβ-null mice will be described elsewhere (K.Sa. and K.A., unpublished data).

All animal experiments were carried out in accordance with the regulations and guidelines for the care and use of experimental animals at the University of Tokyo and were approved

by the institutional review committee of the University of Tokyo Graduate School of Medicine.

Primary neuronal cultures

Hippocampal neurons were prepared from the CA1/CA3 regions of the hippocampus of 1-day-old (P1) SD rats as described elsewhere (Bito et al., 1996; Kawashima et al., 2009). At 14-24 days in vitro (div), the cells were incubated in a growth medium containing TTX (2 μM, Wako, Osaka, Japan) for 24 h. The neurons were then treated with BDNF (50 ng/ml, generously provided by Dainippon Sumitomo Pharma Co., Ltd., Osaka, Japan) for 2 h, further treated with a medium containing channel blockers or inhibitors, and then fixed for immunostaining.

Purification of recombinant proteins and in vitro binding

Bacterially expressed recombinant GST-Arc was purified with glutathione-sepharose 4B beads (GE Healthcare). Recombinant CaMKII and its mutant proteins were expressed in HEK293T cells and purified with calmodulin-sepharose 4B beads (GE Healthcare). Detailed protocols for *in vitro* binding assays are provided in the Extended Experimental Procedures.

Image acquisition and analyses of immunostained neurons

All image acquisition and analyses were performed in a blind manner. Confocal z-stack fluorescence images were obtained using a LSM510 confocal laser microscopy system (Carl Zeiss). All stacked images were projected into single planes by summation and used for quantitative analyses as described below.

For the evaluation of Arc localization in the PSD, PSD spots were defined on the basis of PSD-95 IR clustering essentially as described previously (Nonaka et al., 2006). All PSD-95 spots that were well-separated from the dendritic shaft of an Arc-IR-positive dendrite were analyzed, and a corresponding non-PSD area that was adjacent to a given PSD spot was defined within dendritic shafts for each PSD spot. After background subtraction, the average intensity of Arc immunofluorescence was measured. The intensity ratio of PSD to non-PSD was designated as the Arc accumulation index.

For RNAi and rescue experiments, dendritic segments of GFP (a marker of the shRNA vectors) and Arc double-positive neurons were imaged. Dendritic spine accumulation was evaluated by analyzing the fluorescence-intensity profiles at spine and shaft in dendrites. The spine index for Arc was defined as follows:

Spine index = (Arc-IR peak intensity in spine/Arc-IR peak intensity in shaft)/(GFP-IR peak intensity in spine/GFP-IR peak intensity in shaft). Detailed procedures are provided in the Extended Experimental Procedures.

Live imaging and data analysis

Hippocampal neurons plated on glass-bottom dishes (MatTek) were co-transfected with the pGL4.11-Arc7000-mEGFP-Arc-UTRs and a marker plasmid pTagRFP-C (Evrogen), at 7-9 div. Series of z-stack images for both GFP and RFP signals were acquired at 16-22 div. The

z-stack images were projected into a single-plane image by summation, and the fluorescence line profiles of spines and adjacent dendritic shafts were measured. An index for spine accumulation was defined as follows:

$$\text{Spine index} = (\text{GFP}_{\text{spine}}/\text{GFP}_{\text{shaft}}) / (\text{RFP}_{\text{spine}}/\text{RFP}_{\text{shaft}}),$$

where $\text{GFP}_{\text{spine}}$ and $\text{GFP}_{\text{shaft}}$ represent the peak green fluorescent intensities, while $\text{RFP}_{\text{spine}}$ and $\text{RFP}_{\text{shaft}}$ indicate the peak red fluorescent intensities in the spine and the shaft, respectively. The ratios of spine indices before and 2 h after follow-up incubation of individual spine-shaft pairs were calculated for a cumulative frequency presentation. Arc/CaMKII dual-imaging was done in neurons transfected with pGL4.11-Arc7000-mCherry-Arc-UTRs and pcDNA3-mEGFP-CaMKIIβ. Detailed procedures are provided in the Extended Experimental Procedures.

Surface AMPA-R labeling

Extracellular AMPA-Rs were labeled in live hippocampal neurons (17-18 div) using an anti-GluA1 antibody (Alomone Labs), essentially as described previously (Chowdhury et al., 2006; Shepherd et al., 2006).

The quantification of surface GluA1 puncta was carried out using a custom-made macro running on MetaMorph software (Universal Imaging). All image analyses were performed by a person who was blinded to the experimental conditions. Detailed procedures are provided in the Extended Experimental Procedures.

Statistical analysis

Statistical analyses were performed using Prism 5.0 (GraphPad Software), Excel (Microsoft), MatLab (Mathworks) or JMP 8 (SAS institute). Log-transformation was applied to correct possible skewness of data distribution where appropriate. All data are expressed as the mean ± standard error of the means (s.e.m), unless indicated otherwise.

Supplementary Material

Refer to Web version on PubMed Central for supplementary material.

Acknowledgments

We thank H. Schulman and T. Meyer for several CaMKII constructs, R.Y. Tsien for mCherry cDNA, A. Miyawaki for Venus cDNA, M. Yamamoto for GFP-TeNT cDNA, K.U. Bayer for pmEGFP-CaMKIIβe cDNA, and M. Watanabe for an anti-vGlut1 antibody, and all members of the Bito laboratory for support. BDNF was provided by Dainippon Sumitomo Pharma Co., Ltd., Osaka, Japan. We thank T. Bonhoeffer, K. Deisseroth, R.G.M. Morris, V. Naegerl, R. Redondo, M. van Rossum, M. Schnitzer and R.W. Tsien for valuable comments on an earlier version of this work, and R. Huganir for critical reading of the manuscript. We are indebted to Y. Kondo, K. Saiki., A. Adachi-Morishima, R. Gyobu, and T. Kinbara for assistance. This work was supported in part by Grants-in-Aid (WAKATE, KIBAN, START) from JSPS and MEXT of Japan (to H.O., M.N., S.T-K., K.Sa., and H.B.), from the MHLW of Japan (to H.O. and H.B.), by a grant from NIMH (to P.F.W.), and by awards from the HFSP (to H.O., and H.B.) and the Mitsubishi Foundation (to H.B.). Y.I., N.Y-K., K.S., and T.K. are JSPS predoctoral fellows.

References

Béïque JC, Na Y, Kuhl D, Worley PF, Huganir RL. Arc-dependent synapse-specific homeostatic plasticity. Proc Natl Acad Sci U S A. 2011; 108:816–821. [PubMed: 21187403]

Bito H, Deisseroth K, Tsien RW. CREB phosphorylation and dephosphorylation: a Ca^{2+}- and stimulus duration-dependent switch for hippocampal gene expression. Cell. 1996; 87:1203–1214. [PubMed: 8980227]

Borgesius NZ, van Woerden GM, Buitendijk GH, Keijzer N, Jaarsma D, Hoogenraad CC, Elgersma Y. betaCaMKII plays a nonenzymatic role in hippocampal synaptic plasticity and learning by targeting alphaCaMKII to synapses. J Neurosci. 2011; 31:10141–10148. [PubMed: 21752990]

Caldeira MV, Melo CV, Pereira DB, Carvalho R, Correia SS, Backos DS, Carvalho AL, Esteban JA, Duarte CB. Brain-derived neurotrophic factor regulates the expression and synaptic delivery of alpha-amino-3-hydroxy-5-methyl-4-isoxazole propionic acid receptor subunits in hippocampal neurons. J Biol Chem. 2007; 282:12619–12628. [PubMed: 17337442]

Chowdhury S, Shepherd JD, Okuno H, Lyford G, Petralia RS, Plath N, Kuhl D, Huganir RL, Worley PF. Arc/Arg3.1 interacts with the endocytic machinery to regulate AMPA receptor trafficking. Neuron. 2006; 52:445–459. [PubMed: 17088211]

Donai H, Sugiura H, Ara D, Yoshimura Y, Yamagata K, Yamauchi T. Interaction of Arc with CaM kinase II and stimulation of neurite extension by Arc in neuroblastoma cells expressing CaM kinase II. Neuroscience research. 2003; 47:399–408. [PubMed: 14630344]

Flavell SW, Cowan CW, Kim TK, Greer PL, Lin Y, Paradis S, Griffith EC, Hu LS, Chen C, Greenberg ME. Activity-dependent regulation of MEF2 transcription factors suppresses excitatory synapse number. Science. 2006; 311:1008–1012. [PubMed: 16484497]

Frey U, Morris RG. Synaptic tagging and long-term potentiation. Nature. 1997; 385:533–536. [PubMed: 9020359]

Greer PL, Hanayama R, Bloodgood BL, Mardinly AR, Lipton DM, Flavell SW, Kim TK, Griffith EC, Waldon Z, Maehr R, et al. The Angelman Syndrome protein Ube3A regulates synapse development by ubiquitinating arc. Cell. 2010; 140:704–716. [PubMed: 20211139]

Guzowski JF, Lyford GL, Stevenson GD, Houston FP, McGaugh JL, Worley PF, Barnes CA. Inhibition of activity-dependent arc protein expression in the rat hippocampus impairs the maintenance of long-term potentiation and the consolidation of long-term memory. J Neurosci. 2000; 20:3993–4001. [PubMed: 10818134]

Guzowski JF, McNaughton BL, Barnes CA, Worley PF. Environment-specific expression of the immediate-early gene Arc in hippocampal neuronal ensembles. Nat Neurosci. 1999; 2:1120–1124. [PubMed: 10570490]

Hudmon A, Schulman H. Neuronal CA2+/calmodulin-dependent protein kinase II: the role of structure and autoregulation in cellular function. Annu Rev Biochem. 2002; 71:473–510. [PubMed: 12045104]

Kawashima T, Okuno H, Nonaka M, Adachi-Morishima A, Kyo N, Okamura M, Takemoto-Kimura S, Worley PF, Bito H. Synaptic activity-responsive element in the Arc/Arg3.1 promoter essential for synapse-to-nucleus signaling in activated neurons. Proc Natl Acad Sci U S A. 2009; 106:316–321. [PubMed: 19116276]

Link W, Konietzko U, Kauselmann G, Krug M, Schwanke B, Frey U, Kuhl D. Somatodendritic expression of an immediate early gene is regulated by synaptic activity. Proc Natl Acad Sci U S A. 1995; 92:5734–5738. [PubMed: 7777577]

Lyford GL, Yamagata K, Kaufmann WE, Barnes CA, Sanders LK, Copeland NG, Gilbert DJ, Jenkins NA, Lanahan AA, Worley PF. Arc, a growth factor and activity-regulated gene, encodes a novel cytoskeleton-associated protein that is enriched in neuronal dendrites. Neuron. 1995; 14:433–445. [PubMed: 7857651]

Matsuzaki M, Honkura N, Ellis-Davies GC, Kasai H. Structural basis of long-term potentiation in single dendritic spines. Nature. 2004; 429:761–766. [PubMed: 15190253]

McCurry CL, Shepherd JD, Tropea D, Wang KH, Bear MF, Sur M. Loss of Arc renders the visual cortex impervious to the effects of sensory experience or deprivation. Nat Neurosci. 2010; 13:450–457. [PubMed: 20228806]

Messaoudi E, Kanhema T, Soule J, Tiron A, Dagyte G, da Silva B, Bramham CR. Sustained Arc/Arg3.1 synthesis controls long-term potentiation consolidation through regulation of local actin polymerization in the dentate gyrus in vivo. J Neurosci. 2007; 27:10445–10455. [PubMed: 17898216]

Miller S, Yasuda M, Coats JK, Jones Y, Martone ME, Mayford M. Disruption of dendritic translation of CaMKIIalpha impairs stabilization of synaptic plasticity and memory consolidation. Neuron. 2002; 36:507–519. [PubMed: 12408852]

Mishina M, Sakimura K. Conditional gene targeting on the pure C57BL/6 genetic background. Neuroscience research. 2007; 58:105–112. [PubMed: 17298852]

Moga DE, Calhoun ME, Chowdhury A, Worley P, Morrison JH, Shapiro ML. Activity-regulated cytoskeletal-associated protein is localized to recently activated excitatory synapses. Neuroscience. 2004; 125:7–11. [PubMed: 15051140]

Navakkode S, Sajikumar S, Frey JU. The type IV-specific phosphodiesterase inhibitor rolipram and its effect on hippocampal long-term potentiation and synaptic tagging. J Neurosci. 2004; 24:7740–7744. [PubMed: 15342741]

Nedivi E, Hevroni D, Naot D, Israeli D, Citri Y. Numerous candidate plasticity-related genes revealed by differential cDNA cloning. Nature. 1993; 363:718–722. [PubMed: 8515813]

Nonaka M, Doi T, Fujiyoshi Y, Takemoto-Kimura S, Bito H. Essential contribution of the ligand-binding beta B/beta C loop of PDZ1 and PDZ2 in the regulation of postsynaptic clustering, scaffolding, and localization of postsynaptic density-95. J Neurosci. 2006; 26:763–774. [PubMed: 16421296]

O'Leary H, Lasda E, Bayer KU. CaMKIIbeta association with the actin cytoskeleton is regulated by alternative splicing. Molecular biology of the cell. 2006; 17:4656–4665. [PubMed: 16928958]

Okada D, Ozawa F, Inokuchi K. Input-specific spine entry of soma-derived Vesl-1S protein conforms to synaptic tagging. Science. 2009; 324:904–909. [PubMed: 19443779]

Okamoto K, Narayanan R, Lee SH, Murata K, Hayashi Y. The role of CaMKII as an F-actin-bundling protein crucial for maintenance of dendritic spine structure. Proc Natl Acad Sci U S A. 2007; 104:6418–6423. [PubMed: 17404223]

Park S, Park JM, Kim S, Kim JA, Shepherd JD, Smith-Hicks CL, Chowdhury S, Kaufmann W, Kuhl D, Ryazanov AG, et al. Elongation factor 2 and fragile X mental retardation protein control the dynamic translation of Arc/Arg3.1 essential for mGluR-LTD. Neuron. 2008; 59:70–83. [PubMed: 18614030]

Peebles CL, Yoo J, Thwin MT, Palop JJ, Noebels JL, Finkbeiner S. Arc regulates spine morphology and maintains network stability in vivo. Proc Natl Acad Sci U S A. 2010; 107:18173–18178. [PubMed: 20921410]

Plath N, Ohana O, Dammermann B, Errington ML, Schmitz D, Gross C, Mao X, Engelsberg A, Mahlke C, Welzl H, et al. Arc/Arg3.1 is essential for the consolidation of synaptic plasticity and memories. Neuron. 2006; 52:437–444. [PubMed: 17088210]

Ploski JE, Pierre VJ, Smucny J, Park K, Monsey MS, Overeem KA, Schafe GE. The activity-regulated cytoskeletal-associated protein (Arc/Arg3.1) is required for memory consolidation of pavlovian fear conditioning in the lateral amygdala. J Neurosci. 2008; 28:12383–12395. [PubMed: 19020031]

Qian Z, Gilbert ME, Colicos MA, Kandel ER, Kuhl D. Tissue-plasminogen activator is induced as an immediate-early gene during seizure, kindling and long-term potentiation. Nature. 1993; 361:453–457. [PubMed: 8429885]

Ramirez-Amaya V, Vazdarjanova A, Mikhael D, Rosi S, Worley PF, Barnes CA. Spatial exploration-induced Arc mRNA and protein expression: evidence for selective, network-specific reactivation. J Neurosci. 2005; 25:1761–1768. [PubMed: 15716412]

Redondo RL, Okuno H, Spooner PA, Frenguelli BG, Bito H, Morris RG. Synaptic tagging and capture: differential role of distinct calcium/calmodulin kinases in protein synthesis-dependent long-term potentiation. J Neurosci. 2010; 30:4981–4989. [PubMed: 20371818]

Rial Verde EM, Lee-Osbourne J, Worley PF, Malinow R, Cline HT. Increased expression of the immediate-early gene arc/arg3.1 reduces AMPA receptor-mediated synaptic transmission. Neuron. 2006; 52:461–474. [PubMed: 17088212]

Shen K, Meyer T. In vivo and in vitro characterization of the sequence requirement for oligomer formation of Ca2+/calmodulin-dependent protein kinase IIalpha. J Neurochem. 1998; 70:96–104. [PubMed: 9422351]

Shepherd JD, Rumbaugh G, Wu J, Chowdhury S, Plath N, Kuhl D, Huganir RL, Worley PF. Arc/Arg3.1 mediates homeostatic synaptic scaling of AMPA receptors. Neuron. 2006; 52:475–484. [PubMed: 17088213]

Smith-Hicks C, Xiao B, Deng R, Ji Y, Zhao X, Shepherd JD, Posern G, Kuhl D, Huganir RL, Ginty DD, et al. SRF binding to SRE 6.9 in the Arc promoter is essential for LTD in cultured Purkinje cells. Nat Neurosci. 2010; 13:1082–1089. [PubMed: 20694003]

Steward O, Wallace CS, Lyford GL, Worley PF. Synaptic activation causes the mRNA for the IEG Arc to localize selectively near activated postsynaptic sites on dendrites. Neuron. 1998; 21:741–751. [PubMed: 9808461]

Wang KH, Majewska A, Schummers J, Farley B, Hu C, Sur M, Tonegawa S. In vivo two-photon imaging reveals a role of arc in enhancing orientation specificity in visual cortex. Cell. 2006; 126:389–402. [PubMed: 16873068]

Waung MW, Pfeiffer BE, Nosyreva ED, Ronesi JA, Huber KM. Rapid translation of Arc/Arg3.1 selectively mediates mGluR-dependent LTD through persistent increases in AMPAR endocytosis rate. Neuron. 2008; 59:84–97. [PubMed: 18614031]

Worley PF, Bhat RV, Baraban JM, Erickson CA, McNaughton BL, Barnes CA. Thresholds for synaptic activation of transcription factors in hippocampus: correlation with long-term enhancement. J Neurosci. 1993; 13:4776–4786. [PubMed: 8229198]

Yamamoto M, Wada N, Kitabatake Y, Watanabe D, Anzai M, Yokoyama M, Teranishi Y, Nakanishi S. Reversible suppression of glutamatergic neurotransmission of cerebellar granule cells in vivo by genetically manipulated expression of tetanus neurotoxin light chain. J Neurosci. 2003; 23:6759–6767. [PubMed: 12890769]

Ying SW, Futter M, Rosenblum K, Webber MJ, Hunt SP, Bliss TV, Bramham CR. Brain-derived neurotrophic factor induces long-term potentiation in intact adult hippocampus: requirement for ERK activation coupled to CREB and upregulation of Arc synthesis. J Neurosci. 2002; 22:1532–1540. [PubMed: 11880483]

Highlights

- Arc/Arg3.1 binds to an inactive, rather than active, form of synaptic CaMKIIβ.
- Activity-induced Arc/Arg3.1 accumulates at spines during synaptic inactivity.
- Synaptic Arc/Arg3.1 reduces surface AMPA-R levels in individual spines.
- “Inverse” synaptic tagging may also be critical for late-phase synaptic plasticity.

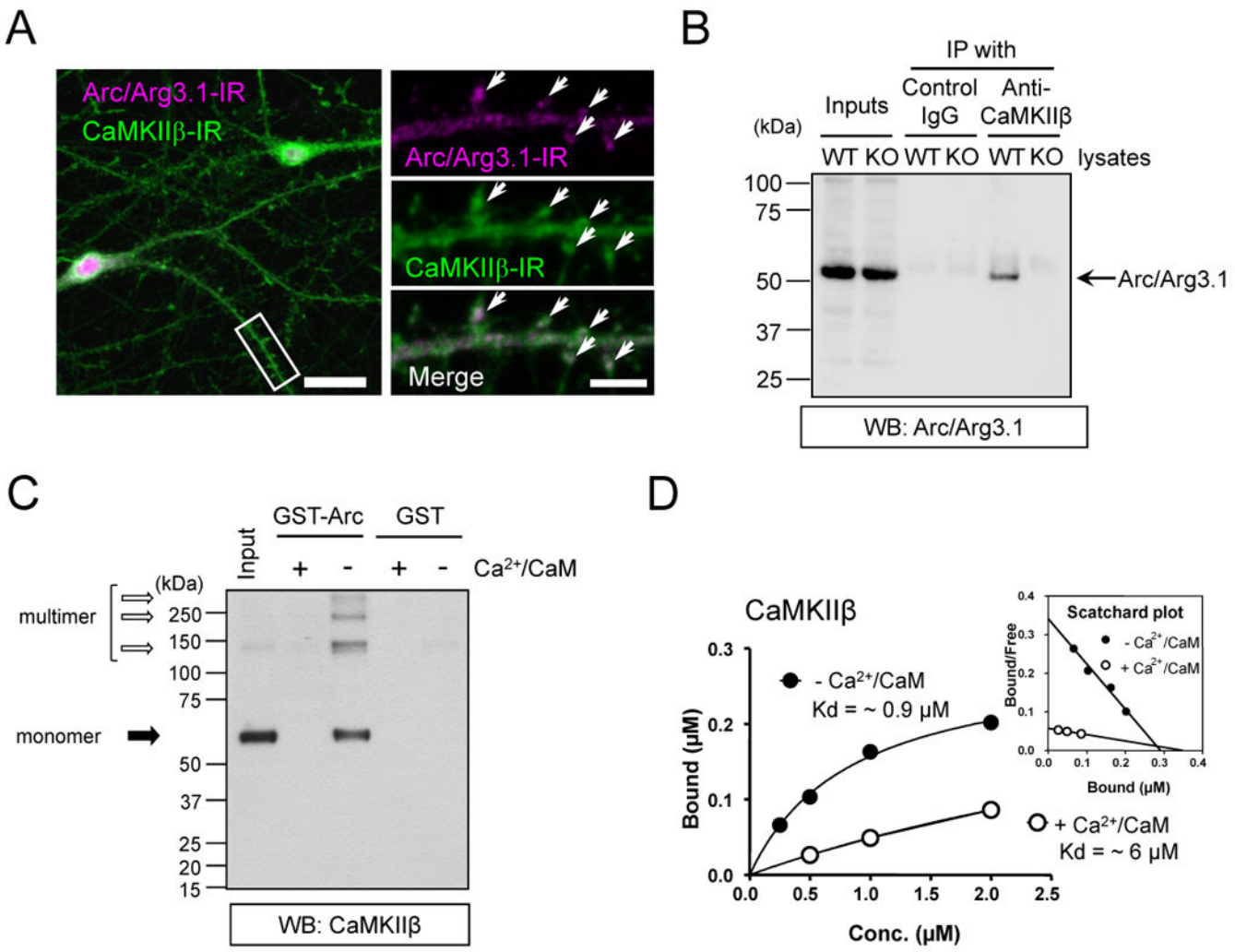

Figure 1. Arc interacts with the beta isoform of CaMKII

(A) Colocalization of Arc with CaMKIIβ in dendritic spines. A dendritic segment of a representative cell (left) is expanded and shown in a frame (right). Arrows represent spines containing both Arc-IR and CaMKIIβ-IR. Scale bars, 20 μm (left) and 5 μm (middle). **(B)** Co-immunoprecipitation of Arc and CaMKIIβ in brain synaptosomal fractions. **(C)** GST pulldown experiments revealed a stringent calcium dependency for Arc-CaMKIIβ binding, which was suppressed when both Ca^{2+} and CaM were present. **(D)** Scatchard analysis confirms strong binding of Arc to CaM-unbound CaMKIIβ (- Ca^{2+}/CaM) and a reduced binding upon CaMKIIβ activation (+ Ca^{2+}/CaM).

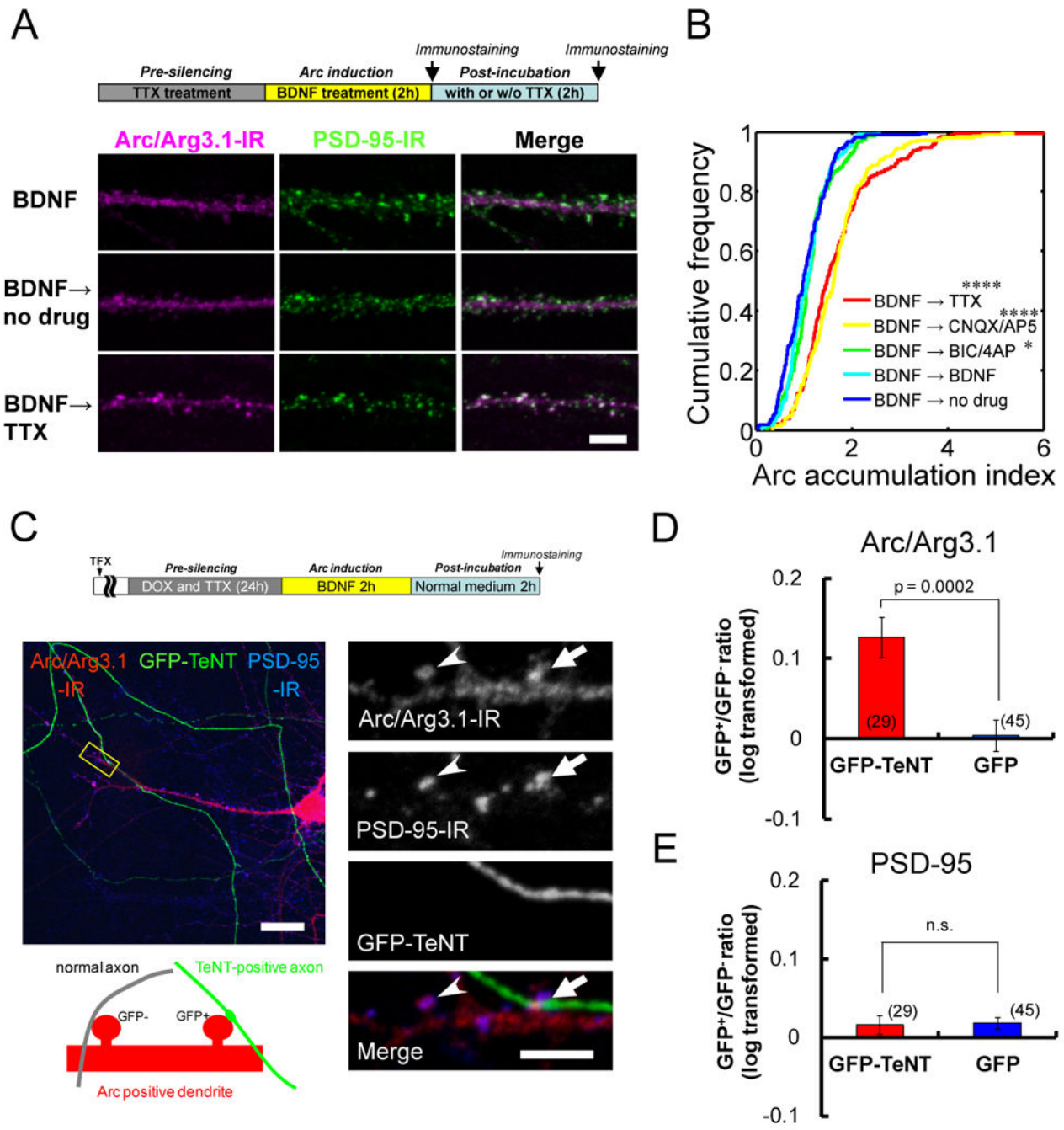

Figure 2. The spine localization of Arc is modulated by synaptic inactivity

(A) Dendrites immunostained for Arc and PSD-95, in neurons pretreated with TTX for 16-24 h, activated with BDNF for 2 h and further incubated with or without TTX for 2 h, as shown by a schematic diagram on the top. Scale bar, 5 μm. **(B)** Arc accumulation index (see Experimental procedures) under various post-activation conditions. *, $p < 0.05$; ****, $p < 0.0001$, in comparison to the no-drug control, K-S test. See also Figure S2C. **(C)** Single-synapse activity blockade by presynaptic expression of a doxycycline-inducible tetanus toxin light chain (TeNT) results in inactive synapse-selective enhancement of Arc. Note that

intense Arc-IR signal was observed in the spine attached to the GFP-TeNT-expressing axon (arrows), as compared to neighboring spines without GFP-positive fibers (arrowheads). TFX, transfection. Scale bars, 20 μm (left) and 5 μm (right). **(D)** The ratio of Arc intensity in a spine close to the GFP-positive axon and the mean Arc intensity in neighboring spines (GFP^+/GFP^- ratio) was calculated in each dendritic segment. The bars represent the average of log-transformed ratios, and the number of examined dendritic segments are shown in parentheses. **(E)** The GFP^+/GFP^- ratio of PSD-95 did not differ between GFP-TeNT and GFP control conditions. p value based on an unpaired t-test.

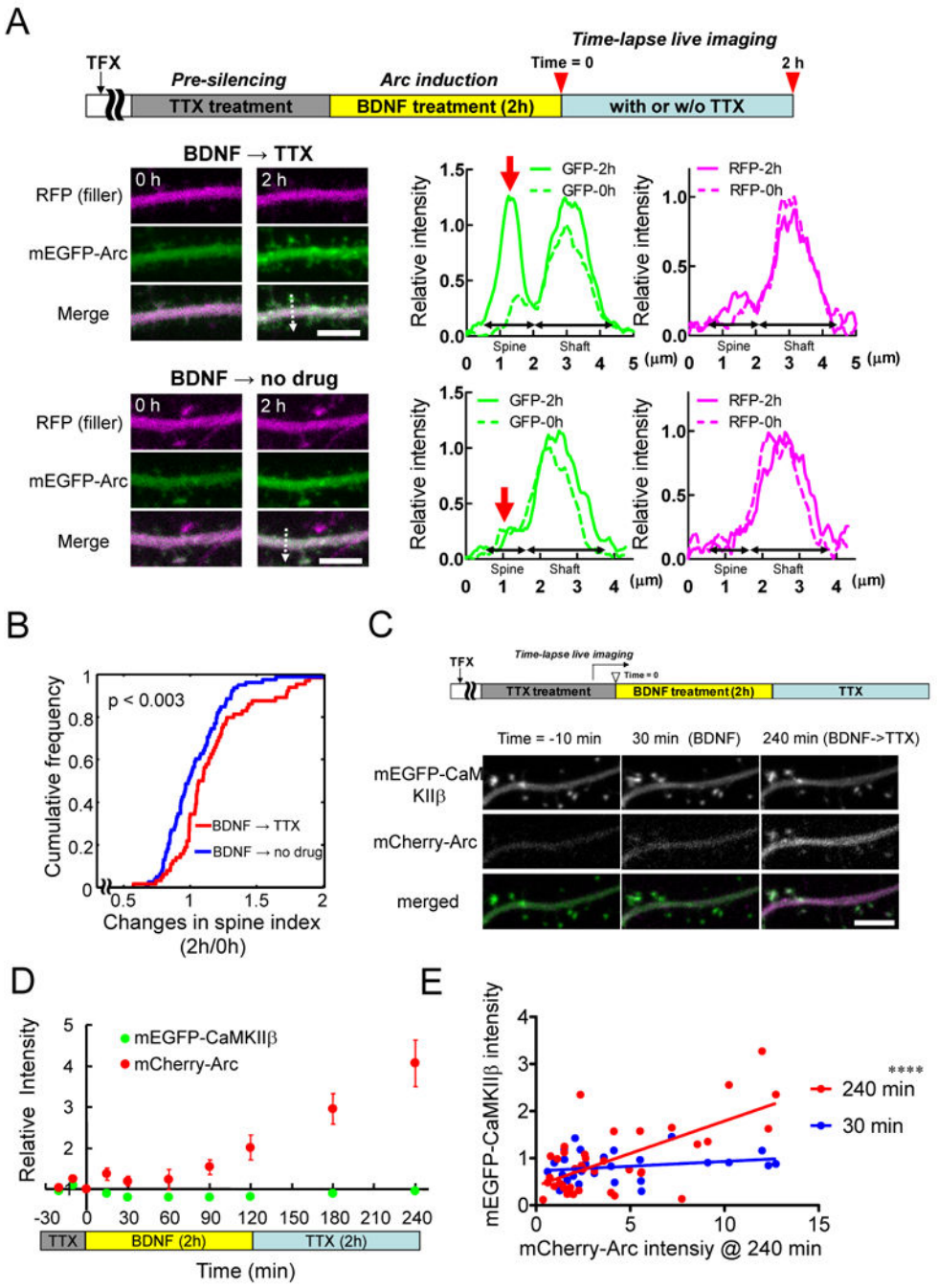

Figure 3. Inactivity-induced synaptic accumulation of Arc in living neurons

(A, B) Live imaging of mEGFP-Arc accumulation in the spines during synaptic inactivity. **(A)** Representative time-lapse images. Red arrows indicate the location of spines analyzed in the line profiles (dotted arrows in left panels). Scale bar, 5 μm. **(B)** A cumulative frequency histogram of spine index changes between 0 and 2 h (see Experimental procedures). **(C-E)** Time-lapse imaging of mEGFP-tagged CaMKIIβ and activity-driven mCherry-Arc. **(C)** A schematic experimental diagram and representative time-lapse images. Recording started before BDNF stimulation. Scale bar, 5 μm. **(D)** Time course of changes in averaged relative

fluorescent intensities in spines. **(E)** Relationship between the intensity of mCherry-Arc at the end of imaging session (240 min) and those of mEGFP-CaMKIIβ at 30 min and at 240 min, in individual spines. ****, $p < 0.0001$.

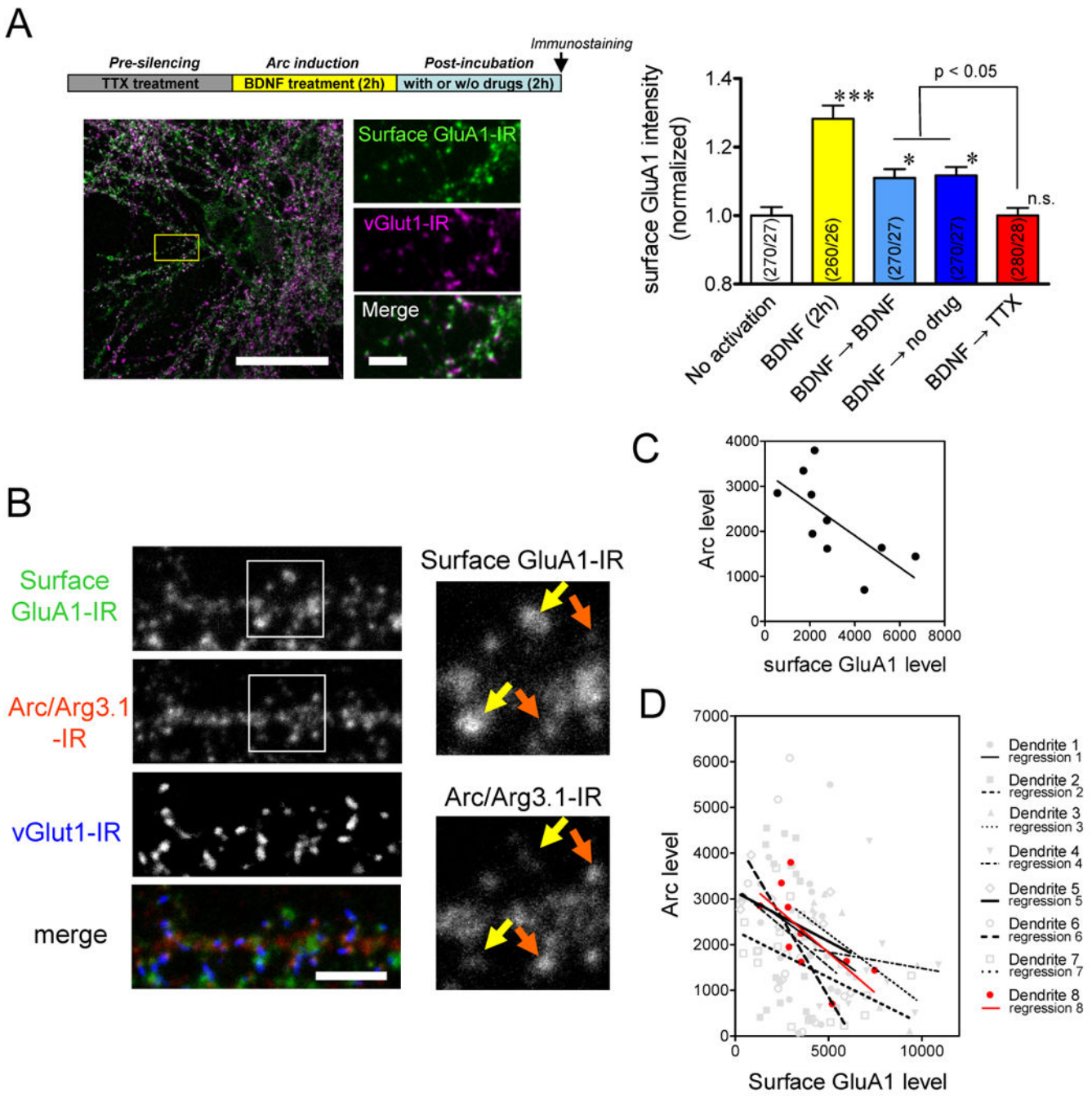

Figure 4. Synaptic Arc content is inversely correlated to surface expression levels of GluA1 in individual synapses

(A) A period of inactivity that promotes synaptic Arc maintenance also results in reduced surface expression levels of GluA1. Left, representative images of surface GluA1 IR juxtaposed to vGlut1 puncta in neurons treated with BDNF followed by TTX. Neurons were first live-stained for surface GluA1 (green) and then stained for vGlut1 (magenta) after fixation. Scale bars, 50 μm (Left) and 5 μm (right). Right, quantification of the average intensity of GluA1 surface staining. *, $p < 0.05$; ***, $p < 0.001$ (compared to the no-

activation control by ANOVA with a Tukey's test). **(B)** Representative triple immunostaining of a dendritic segment from hippocampal neurons treated with BDNF followed by TTX. Framed areas are expanded on the right. Some spines contained high surface GluA1 signals but low Arc signals (yellow arrows), whereas others displayed the opposite pattern (orange arrows). Scale bar, 5 μm. **(C)** Negative correlation of synaptic Arc and surface GluA1 levels at individual synapses. The synaptic GulA1 and Arc levels in the dendritic segment shown in (B) were measured and plotted. **(D)** Population data of the GluA1 and Arc expression analysis. Lines represent the regression lines of individual dendritic segments from 8 cells. Red symbols (Dendrite 8) and line are the same data shown in (C).

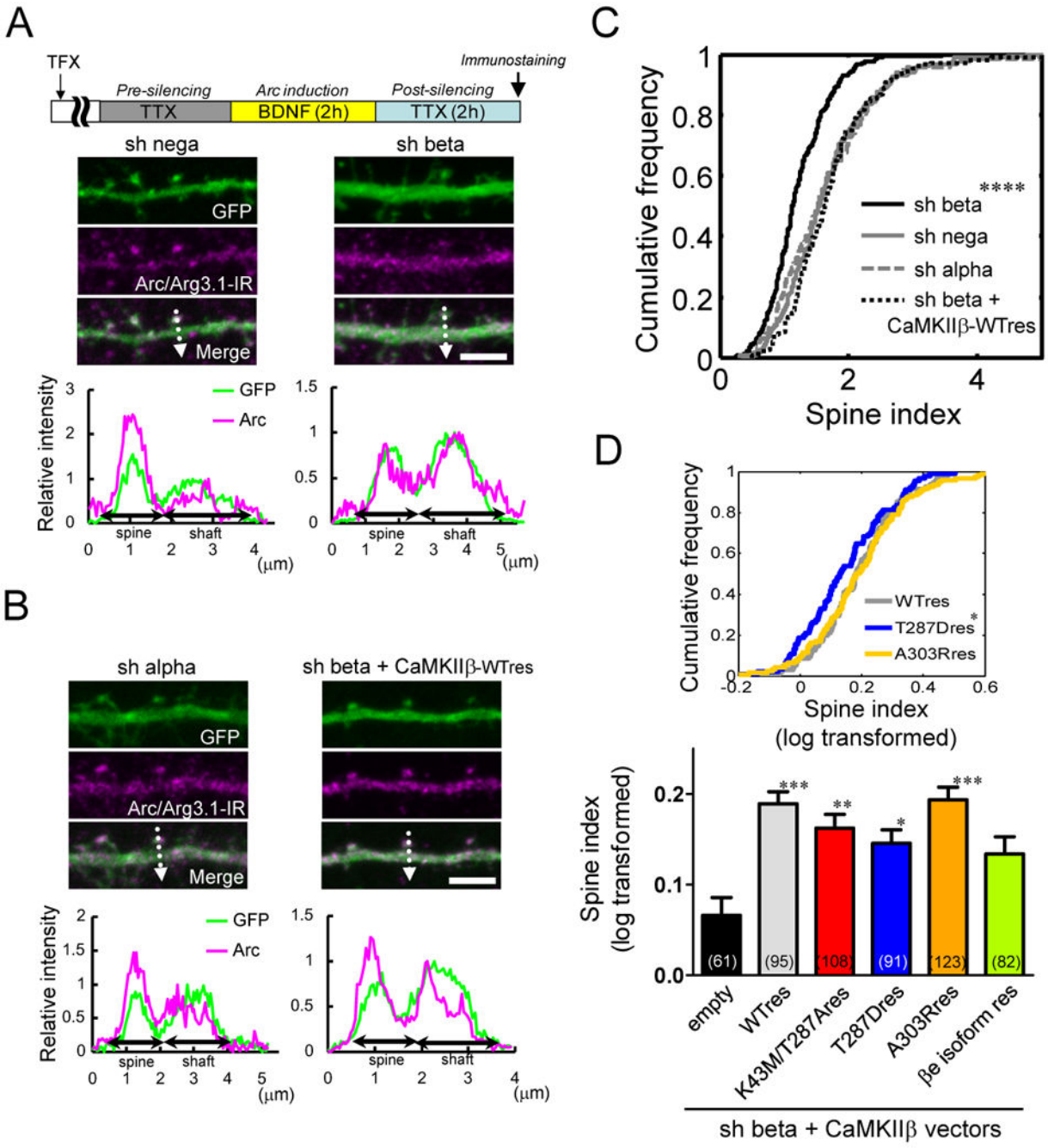

Figure 5. Loss of Arc accumulation in dendritic spines by knockdown of CaMKIIβ but not CaMKIIα

(A) Line profiles of Arc signals in the dendritic spines and shafts of CaMKIIβ knockdown (sh beta) and control (sh nega) neurons. Neurons were prepared and treated as shown in the schematic at the top. Both Arc and GFP signals were independently normalized to their peak intensities in dendritic shafts. Scale bar, 5 μm. **(B)** Line profiles in CaMKIIα knockdown (sh alpha) and "rescued" (sh beta + CaMKIIβ-WTres) neurons. **(C)** The cumulative frequency of the spine index of Arc. ****, $p < 0.0001$ by a K-S test. See also Figure S5A. **(D)** Rescuing

deficit of synaptic Arc accumulation in CaMKIIβ-knockdown neurons using RNAi-resistant CaMKIIβ mutants. Top, cumulative frequency of the spine index for WT and two representative mutants T287D and A303R. The distribution of T287D significantly differs from both WT and A303R by a K-S test ($p < 0.05$). Bottom, a bar graph indicating the average of the spine index. Empty, vector only; WT, wild-type; K43M/T287A, kinase-dead and autophosyphorylation-deficient; T287D, phospho-mimic; A303R, CaM-binding deficient; βe, F-actin-binding deficient; "res" denotes RNAi-resistant. The numbers of spines examined are shown in parentheses. *, $p < 0.05$; **, $p < 0.01$; ***, $p < 0.001$; n.s., $p > 0.05$ by ANOVA with a Tukey's test compared with the empty control.

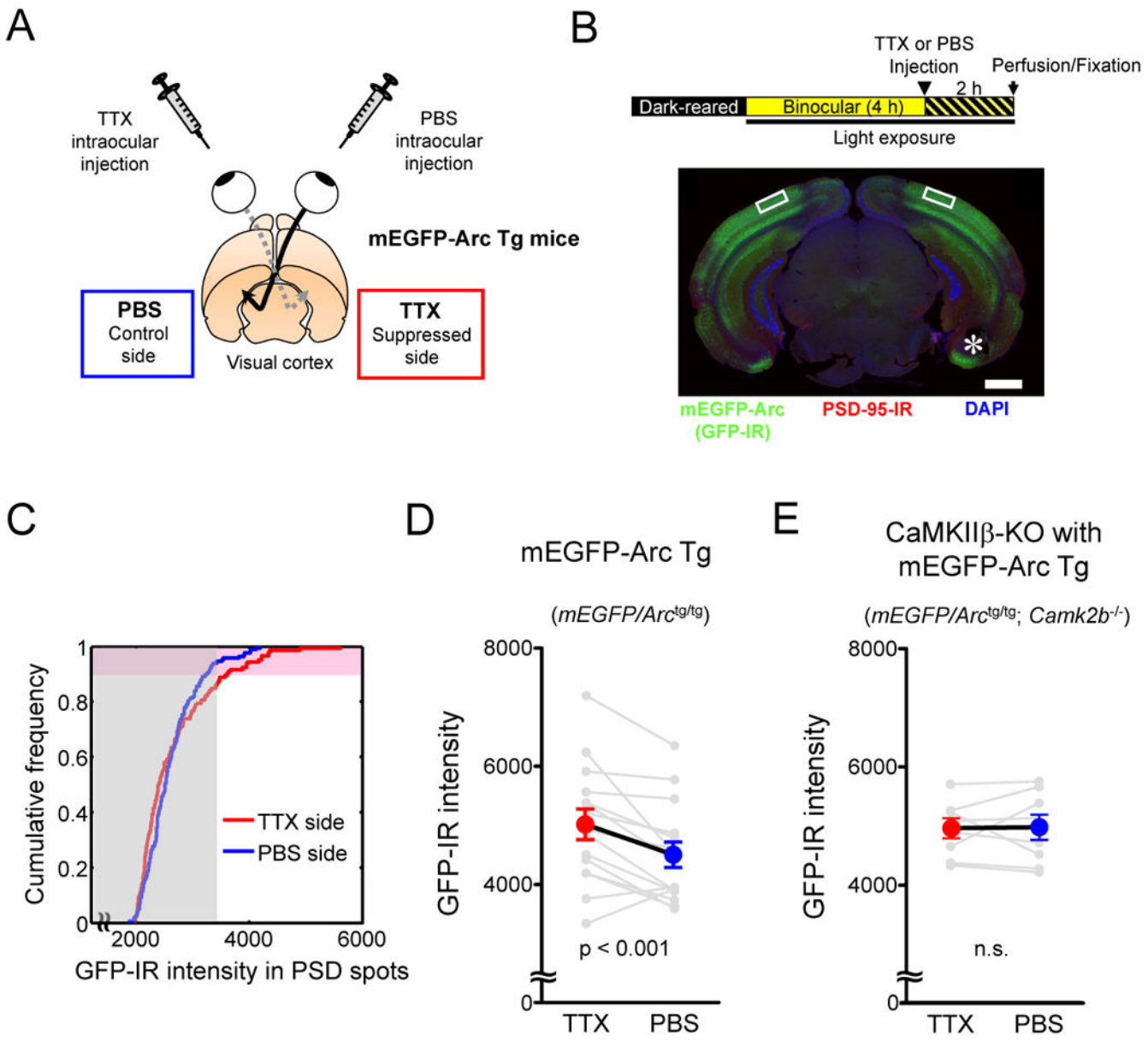

Figure 6. Enhancement of Arc synaptic accumulation with inactivity and its dependency on CaMKIIβ *in vivo*

(A) A schematic drawing of the intra-animal comparison of inactivated and control hemispheres. **(B)** A representative immunohistochemical section of mEGFP-Arc Tg mice underwent unilateral activity suppression after a 4-h light exposure. A schematic paradigm is shown at the top. The layer 2/3 of the monocular zone of the primary visual cortex (boxed areas) was analyzed for quantification. Note that TTX injection after light exposure had little effect on the overall mEGFP-Arc expression (*, suppressed hemisphere). Scale bar, 1mm. **(C)** A representative intra-animal cumulative histogram comparison across hemispheres of mEGFP-Arc intensities in PSD spots. As most mEGFP-Arc signals were below background levels (blue shaded area), the average of the top 10% intensities (pink shaded area) were used for the population analysis in (D). **(D)** Population analysis of the intra-animal

comparisons. The mEGFP-Arc intensities at the TTX-affected side were significantly higher than those of the control side ($p < 0.001$, paired-t test) (N = 15 animals). **(E)** The effect of CaMKIIβ-null genotype on Arc synaptic localization *in vivo*. The enhancement of mEGFP-Arc intensities in the TTX-affected side was abolished in this genotype (N = 8 animals).

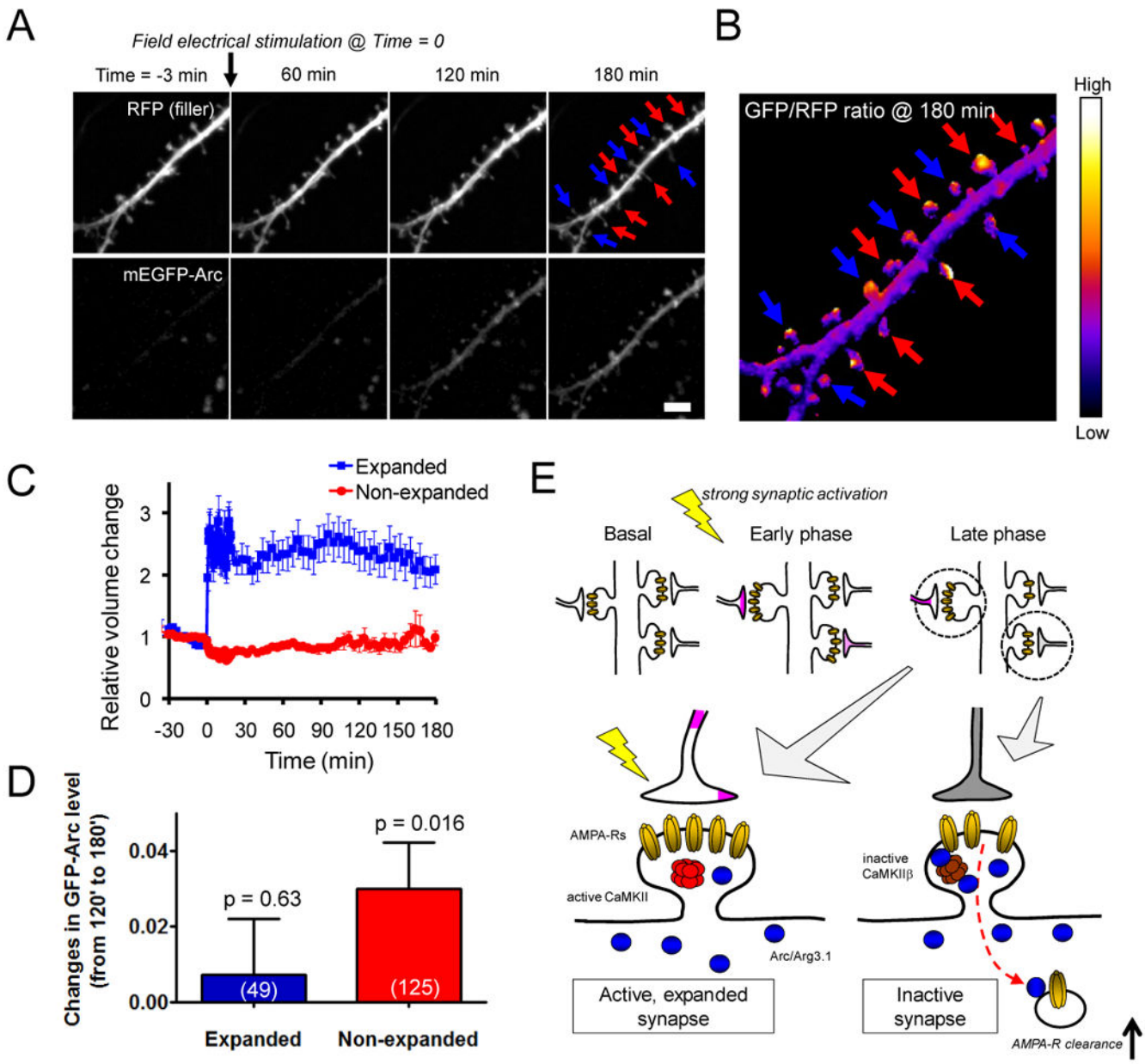

Figure 7. Activity-induced Arc accumulates at non-expanded synapses rather than expanded synapses following structural plasticity-inducing stimulation

(A) Time-lapse images of activity-induced mEGFP-Arc and a volume marker TagRFP following high-frequency field electrical stimulation that induces spine volume expansion. Expanded (blue arrows) and non-expanded (red arrows) spines are illustrated for clarity. Scale bar, 5 μm. **(B)** A pseudocolor GFP/RFP ratio map of the dendritic segment shown in (A) at 180 min after the stimulation. **(C)** In expanded spines, high-frequency electrical stimulation induced long-lasting volume expansion that lasted for at least 3 h after the stimulation, while no apparent changes were observed in non-expanded spines. **(D)** The GFP-Arc levels (shown as the ratio at 180 min and at 120 min, and log-transformed), in non-expanded spines, significantly increased during 120 min to 180 min after the stimulation (p

= 0.016), but not in expanded spines (p = 0.63). **(E)** Arc action on AMPA-R clearance at active and inactive synapses. After synaptic potentiation, the surface AMPA-Rs are augmented at the synapses that receive strong inputs, while a cell-wide Arc induction is also triggered. During the late phase of potentiation, Arc is differently maintained in the synapses depending on the amount and history of synaptic activity. In the synapses that receive frequent inputs (active or late LTP-like synapses), CaMKIIβ is more likely to be activated, and thus its interaction with Arc is largely weakened. As a result, Arc may diffuse out from the synapses more freely. In contrast, synapses with low activity (inactive or early-LTP like synapses) are more likely to contain an inactive form of CaMKIIβ, which provides a scaffold for Arc at the synapse. The CaMKIIβ-stabilized Arc may efficiently contribute to promoting AMPA-R clearance from the inactive synapse. Through such an *in*activity-dependent control of synaptic dynamics, Arc may contribute to synaptic homeostasis and restrict the resident time of newly recruited surface AMPA-Rs at inactive synapses, while active, potentiated synapses remain unaffected.